

Resolving Hubble Tension with Quintom Dark Energy Model

Sirachak Panpanich,^{1,*} Piyabut Burikham,^{1,†} Supakchai Ponglertsakul,^{2,‡} and Lunchakorn Tannukij^{3,§}

¹*High Energy Physics Theory Group, Department of Physics, Faculty of Science,
Chulalongkorn University, Phayathai Rd., Bangkok 10330, Thailand*

²*Department of Physics and Astronomy, Sejong University, Seoul 05006, Republic of Korea*

³*Theoretical and Computational Physics Group, Theoretical and Computational Science Center(TaCS),
Faculty of Science, King Mongkut's University of Technology Thonburi, Prachautid Rd., Bangkok 10140, Thailand*

(Dated: August 12, 2019)

Recent low-redshift observations give value of the present-time Hubble parameter $H_0 \simeq 74$ km/sec/Mpc, roughly 10% higher than the predicted value $H_0 = 67.4$ km/sec/Mpc from Planck's observations of the CMB and the Λ CDM model. Phenomenologically, we show that the Friedmann equation requires an extra unknown component X to contribute a negative density to the Universe in order to resolve the Hubble tension without changing the Planck's constraint on the matter and dark energy densities. For the extra negative density to be sufficiently small, its equation-of-state parameter must satisfy $1/3 \leq w_X \leq 1$. We propose a quintom model of two scalar fields that realizes this condition and successfully resolve the Hubble tension. One scalar field acts as a quintessence while another "phantom" scalar conformally couples to matter in such a way that viable cosmological scenario can be achieved. The model depends only on two parameters, λ_ϕ and δ which represent rolling tendency of the self-interacting potential of the quintessence and the strength of conformal phantom-matter coupling respectively.

PACS numbers:

I. INTRODUCTION

After discovery of the accelerated expansion of the Universe [1, 2], a number of hypotheses have been proposed to solve the dark energy problem, such as Horndeski theories [3–5], generalized proca theories [6, 7], or a ghost-free massive gravity [8, 9]. However, the discovery of gravitational waves GW170817 [10] severely constrains these modified gravity models [11–13]. The simplest standard model of cosmology, without introducing any new gravitational degrees of freedom, is the Λ CDM. With "minimal" proposal of dark matter and dark energy components, it can explain the accelerated expansion of the Universe as well as other observational data reasonably well until recently [14]. A number of low-redshift observations reveals that there are discrepancies between the values of the Hubble parameter at the present time H_0 from observations of Cepheids in the Large Magellanic Cloud (LMC) [15], the gravitational lensing of quasars measurement [16, 17], and the predicted value from the Planck CMB data within the Λ CDM (Note that an intermediate value is found by using Red Giants as the distance ladder [18]). Since the difference between H_0 is roughly 5σ in significance, this means that the standard model of cosmology, the Λ CDM, may not be correct. There exists tension between H_0 predicted from the early Universe and those directly measured at low redshifts.

Many ideas have been proposed to resolve the Hub-

ble tension, such as the galileon gravity model [19], the gravitational [20] and vacuum [21] phase transition, the early dark energy [22], the dark matter decay [23], the neutrino self-interaction [24] and the negative cosmological constant [25]. In this work, we demonstrate that the usual Friedmann equation allows a higher value of $H_0 = 74.03$ km/sec/Mpc while keeping the matter contribution to 31% and the dark energy contribution to 69%, provided that an extra component with very small negative density is introduced. The negative component must be a very small fraction to the total density of the Universe otherwise it would have been detected (see Ref. [26] however, for possible galactic effects of small negative density to the rotation curves). As a theoretical model of such possibility, we propose a modified quintom model [27] to realize a negative-density component required by the Friedmann equation phenomenologically. The quintom model consists of a quintessence scalar field and a phantom scalar field. The model can provide dark energy with phantom crossing, while a late-time solution is still stable. Using two scalar fields for dark energy is not a new novel, a model called a gravitational scalar-tensor theory also possesses two scalar fields [28, 30]. It is interesting to see whether the phantom scalar field of the quintom model matches with the required negative density and could resolve the Hubble tension.

This paper is organized as follows. Section II generally discusses the physical requirement of the extra component X to coexist within the standard Friedmann model in order to resolve the Hubble tension. In Section III we propose a modified quintom model with scalar-matter coupling that realizes the negative density requirement, giving the right H_0 while keeping the density parameters $\Omega_m^{(0)} \simeq 0.31, \Omega_{DE}^{(0)} \simeq 0.69$ consistent with Planck's

*Electronic address: sirachakp-at-gmail.com

†Electronic address: piyabut-at-gmail.com

‡Electronic address: supakchai.p-at-gmail.com

§Electronic address: l'tannukij-at-hotmail.com

early Universe constraints. We use a dynamical system approach to find cosmological solutions of the modified quintom model in Section IV. Section V contains the numerical analysis of the quintom model, yielding realistic cosmological solution. Section VI compares theoretical prediction of our model with the observational data and Section VII summarizes our work.

II. GENERAL PHENOMENOLOGY

In this section, a general physical condition is discussed based on the Friedmann equation with one extra component in addition to the standard Λ CDM model. In this approach it is assumed that the Planck's constraints from the early Universe on H_0 is valid, i.e., $\Omega_m^{(0)} = 0.31, \Omega_\Lambda^{(0)} = 0.69$ and very small contributions from other components at the present day.

Using a density parameter, $\Omega_i \equiv \rho_i/\rho_c$, where $\rho_c \equiv 3H^2/8\pi G$ is the critical density of the Universe, the generalized Friedmann equation for the spatially flat Universe is given by

$$H^2(z) = H_0^2 \left[\Omega_r^{(0)}(1+z)^4 + \Omega_m^{(0)}(1+z)^3 + \Omega_{DE}^{(0)} \exp \left(3 \int_0^z \frac{1+w_{DE}(z)}{1+z} dz \right) + \Omega_X^{(0)} \exp \left(3 \int_0^z \frac{1+w_X(z)}{1+z} dz \right) \right], \quad (2.1)$$

where the subscript r, m, DE, X represents radiation, matter, dark energy, and the extra unknown component X respectively. Notation “(0)” denotes the present value at zero redshift. In the Λ CDM model with $w_{DE} = -1$, observational data from the CMB and high-redshifts prefers $\Omega_m^{(0)} = 0.308, \Omega_r^{(0)} = 5.38 \times 10^{-5}$, and $\Omega_{\Lambda=DE}^{(0)} = 0.692$, and $H_0 = 67.4$ km/s/Mpc [14, 35]. We can thus calculate $H(z)$ at the last-scattering surface ($z \approx 1100$) to be approximately 1.492149×10^6 km/s/Mpc. In order to address the Hubble tension where the value of H at small z is relatively large compared to the Planck value $H_0 = 67.4$ km/s/Mpc, we use $H(z = 1100) = 1.492149 \times 10^6$ km/s/Mpc and $H_0 = 74.03$ km/s/Mpc to find the physical constraint on the extra unknown component X from Eq. (2.1). The allowed values of $w_X, \Omega_X^{(0)}$ are shown in Fig. 1, assuming the simplest case where w_X is constant.

Remarkably, *negative energy density* $\Omega_X^{(0)} < 0$ is required. According to Fig 1, the negative density cannot be a negative mass ($w_X \approx 0$) otherwise $\Omega_X^{(0)}$ is too large $\Omega_X^{(0)} \simeq -0.06$, and it should have been observed. For $1/3 \leq w_X \leq 1$, however, the amount of the extra component X is very small, i.e., $-0.00005707 \leq \Omega_X^{(0)} \leq -4.708 \times 10^{-11}$. Thus in order to solve the Hubble tension problem we require a negative density with $1/3 \leq w_X \leq 1$ without modification on the CMB observational data.

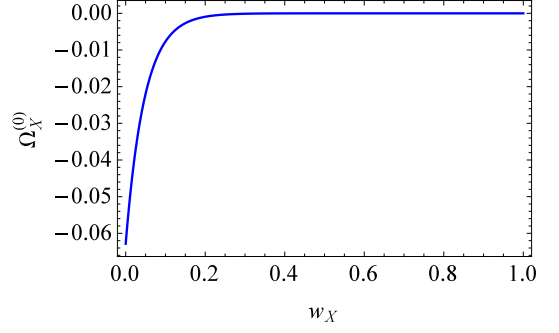


FIG. 1: A relation between $\Omega_X^{(0)}$ and w_X from Eq. (2.1) for $\Omega_m^{(0)} = 0.308, \Omega_r^{(0)} = 5.38 \times 10^{-5}$, and $\Omega_{\Lambda=DE}^{(0)} = 1 - \Omega_r^{(0)} - \Omega_m^{(0)} - \Omega_X^{(0)}, w_{DE} = -1$.

In Section III, a quintom model with two scalars is proposed as a realization of the extra component X . A “phantom” (with negative kinetic energy term) scalar is assumed to couple to matter while the other scalar serves simply as the dark energy responsible for accelerated expansion of the Universe.

III. QUINTOM DARK ENERGY MODEL

We consider the quintom action with 2 scalar fields and interaction between matter fields and one of the scalar field as the following

$$S = \int d^4x \sqrt{-g} \left[\frac{1}{2\kappa^2} R - \frac{1}{2}(\partial\phi)^2 + \frac{1}{2}(\partial\sigma)^2 - V(\phi) \right] + S_M(g_{\mu\nu}, \sigma, \psi_M), \quad (3.1)$$

where $\kappa^2 = 8\pi G$ is an inverse of the reduced Planck mass squared. R is the Ricci scalar, ϕ is a quintessence scalar field, σ is a “phantom” scalar field, and ψ_M is a matter field. We assume that there is only one self-interacting potential of the quintessence scalar field, while the “phantom” scalar field is rolling on an effective potential arising from the phantom-matter interaction as we will explain below. Strictly speaking, this σ is not exactly the standard phantom but rather a ghost field since its equation of state is $P_\sigma = \rho_\sigma < 0$. However, here and henceforth we will simply call it the phantom field for convenience, and also in accordance with the original name quintom (quintessence + phantom). The extra component X is identified with the phantom field σ in this model.

By varying the action with respect to $g^{\mu\nu}$, we obtain the equation of motion

$$R_{\mu\nu} - \frac{1}{2}g_{\mu\nu}R = \kappa^2(T_{\mu\nu}^{(M)} + T_{\mu\nu}^{(\phi)} + T_{\mu\nu}^{(\sigma)}), \quad (3.2)$$

where $T_{\mu\nu}^{(M)}$ is an energy-momentum tensor of the non-relativistic matter and radiation. Energy-momentum

tensors of the quintessence scalar field and the phantom scalar field are given by

$$T_{\mu\nu}^{(\phi)} = \partial_\mu \phi \partial_\nu \phi + g_{\mu\nu} \left(-\frac{1}{2}(\partial\phi)^2 - V(\phi) \right), \quad (3.3)$$

$$T_{\mu\nu}^{(\sigma)} = -\partial_\mu \sigma \partial_\nu \sigma + g_{\mu\nu} \left(\frac{1}{2}(\partial\sigma)^2 \right), \quad (3.4)$$

respectively. Using the flat Friedmann-Lemaître-Robertson-Walker (FLRW) metric, $ds^2 = -dt^2 + a^2(t)d\mathbf{x}^2$, and assuming $\phi = \phi(t)$ and $\sigma = \sigma(t)$, we obtain the Friedmann equations,

$$3H^2 = \kappa^2(\rho_m + \rho_r + \rho_\phi + \rho_\sigma), \quad (3.5)$$

$$3H^2 + 2\dot{H} = \kappa^2(-P_m - P_r - P_\phi - P_\sigma). \quad (3.6)$$

ρ_m , ρ_r , P_m , and P_r are energy densities and pressures of non-relativistic matter and radiation, respectively. The notation “ \cdot ” means a derivative with respect to time. The energy densities and pressures of the scalar fields are

$$\rho_\phi = \frac{1}{2}\dot{\phi}^2 + V(\phi), \quad \rho_\sigma = -\frac{1}{2}\dot{\sigma}^2, \quad (3.7)$$

$$P_\phi = \frac{1}{2}\dot{\phi}^2 - V(\phi), \quad P_\sigma = -\frac{1}{2}\dot{\sigma}^2. \quad (3.8)$$

We then can define an equation of state parameter of the dark energy and an effective equation of state parameter as

$$w_{DE} \equiv \frac{P_\phi + P_\sigma}{\rho_\phi + \rho_\sigma} = \frac{\frac{1}{2}\dot{\phi}^2 - \frac{1}{2}\dot{\sigma}^2 - V(\phi)}{\frac{1}{2}\dot{\phi}^2 - \frac{1}{2}\dot{\sigma}^2 + V(\phi)}, \quad (3.9)$$

$$w_{\text{eff}} \equiv \frac{P_\phi + P_\sigma + P_m + P_r}{\rho_\phi + \rho_\sigma + \rho_m + \rho_r} = -1 - \frac{2}{3} \frac{\dot{H}}{H^2}. \quad (3.10)$$

For each scalar field, their equation of state parameters are

$$w_\phi = \frac{P_\phi}{\rho_\phi} = \frac{\frac{1}{2}\dot{\phi}^2 - V(\phi)}{\frac{1}{2}\dot{\phi}^2 + V(\phi)}, \quad w_\sigma = \frac{P_\sigma}{\rho_\sigma} = +1. \quad (3.11)$$

Note that ρ_σ is negative, and w_σ is always equal to +1. These are crucial in resolving the Hubble tension problem which we will show in the Section IV.

We assume there is only an interaction between matter field and the phantom field, i.e. $\nabla_\mu T_\nu^{\mu(\phi)} = 0$. In this work we consider the interaction in the form

$$\nabla_\mu T_\nu^{\mu(M)} = \kappa \delta T_M \nabla_\nu \sigma, \quad (3.12)$$

$$\nabla_\mu T_\nu^{\mu(\sigma)} = -\kappa \delta T_M \nabla_\nu \sigma, \quad (3.13)$$

where $T_M = -\rho_M + 3P_M$, and δ is a dimensionless constant. This is a conformal interaction form which arises in many scalar-tensor theories after taking a conformal transformation to the Einstein frame [31, 32]. Hence, the continuity equations are

$$\dot{\rho}_m + 3H\rho_m = \kappa \delta \rho_m \dot{\sigma}, \quad (3.14)$$

$$\dot{\rho}_\sigma + 3H(\rho_\sigma + P_\sigma) = -\kappa \delta \rho_m \dot{\sigma}, \quad (3.15)$$

$$\dot{\rho}_\phi + 3H(\rho_\phi + P_\phi) = 0, \quad (3.16)$$

$$\dot{\rho}_r + 4H\rho_r = 0. \quad (3.17)$$

Substituting energy density and pressure of each scalar field we find the equations of motion

$$\ddot{\sigma} + 3H\dot{\sigma} = \kappa \delta \rho_m, \quad (3.18)$$

$$\ddot{\phi} + 3H\dot{\phi} + V_{,\phi} = 0. \quad (3.19)$$

The RHS of the equation of motion of the phantom scalar field acts as an effective potential. This is similar to the effective potential in the chameleon or symmetron gravity [29, 33, 34] (see Appendix A).

IV. DYNAMICAL SYSTEM

A. Autonomous Equations and Fixed Points

We will use a dynamical system approach to study cosmological scenarios of the quintom dark energy model through the behaviour of their fixed points. First, the dimensionless dynamical variables are defined as the following

$$x_1 \equiv \frac{\kappa \dot{\phi}}{\sqrt{6}H}, \quad x_2 \equiv \frac{\kappa \sqrt{V(\phi)}}{\sqrt{3}H}, \quad x_3 \equiv \frac{\kappa \dot{\sigma}}{\sqrt{6}H}, \quad x_4 \equiv \frac{\kappa \sqrt{\rho_r}}{\sqrt{3}H}. \quad (4.1)$$

According to the Friedmann equation (3.5), the density parameters in terms of the dynamical variables are

$$\Omega_m = 1 - x_1^2 - x_2^2 + x_3^2 - x_4^2, \quad (4.2)$$

$$\Omega_r = x_4^2, \quad (4.3)$$

$$\Omega_{DE} = x_1^2 + x_2^2 - x_3^2, \quad (4.4)$$

$$\Omega_\phi = x_1^2 + x_2^2, \quad (4.5)$$

$$\Omega_\sigma = -x_3^2, \quad (4.6)$$

where $\Omega_m \equiv \kappa^2 \rho_m / 3H^2$. In addition, the equation of states are

$$w_{DE} = \frac{x_1^2 - x_2^2 - x_3^2}{x_1^2 + x_2^2 - x_3^2}, \quad (4.7)$$

$$w_\phi = \frac{x_1^2 - x_2^2}{x_1^2 + x_2^2}, \quad (4.8)$$

$$w_\sigma = 1, \quad (4.9)$$

$$w_{\text{eff}} = -1 + \frac{1}{3} (3 + 3x_1^2 - 3x_2^2 - 3x_3^2 + x_4^2). \quad (4.10)$$

In the last equation we have used the second Friedmann equation (3.6) which leads to

$$\frac{\dot{H}}{H^2} = -\frac{1}{2} (3 + 3x_1^2 - 3x_2^2 - 3x_3^2 + x_4^2). \quad (4.11)$$

Differentiating the dynamical variables with respect to N , where $N = \ln a$ is an e-folding number, we find a set

	x_1	x_2	x_3	x_4	Existence
(a)	$x_1^2 - x_3^2 = 1$	0		0	$x_1^2 - x_3^2 = 1$
(b)	0	0	0	1	All
(c)	0	0	$-\frac{1}{\sqrt{6}\delta}$	$\sqrt{1 + \frac{1}{2\delta^2}}$	All
(d)	0	0	$\sqrt{\frac{2}{3}}\delta$	0	All
(e)	$\frac{2\sqrt{6}}{3\lambda_\phi}$	$\frac{2\sqrt{3}}{3\lambda_\phi}$	0	$\sqrt{1 - \frac{4}{\lambda_\phi^2}}$	$\lambda_\phi \geq 2$
(f)	$\frac{2\sqrt{6}}{3\lambda_\phi}$	$\frac{2\sqrt{3}}{3\lambda_\phi}$	$-\frac{1}{\sqrt{6}\delta}$	$\frac{\sqrt{\lambda_\phi^2 + 2\delta^2(\lambda_\phi^2 - 4)}}{\sqrt{2\delta}\lambda_\phi}$	$0 < \lambda_\phi < 2, 0 < \delta \leq \sqrt{\frac{\lambda_\phi^2}{8 - 2\lambda_\phi^2}}$ or $\lambda_\phi \geq 2, \delta > 0$
(g)	$\frac{\lambda_\phi}{\sqrt{6}}$	$\sqrt{1 - \frac{\lambda_\phi^2}{6}}$	0	0	$0 < \lambda_\phi \leq \sqrt{6}$
(h)	$\frac{(3-2\delta^2)\lambda_\phi}{\sqrt{6}(\lambda_\phi^2 - 2\delta^2)}$	$\sqrt{\frac{-36\delta^2 + 9\lambda_\phi^2 - 4\delta^4(\lambda_\phi^2 - 6)}{6(\lambda_\phi^2 - 2\delta^2)^2}}$	$-\sqrt{\frac{2}{3}}\frac{\delta(\lambda_\phi^2 - 3)}{2\delta^2 - \lambda_\phi^2}$	0	$\delta > 0, \lambda_\phi = \sqrt{3}$ or $\delta > 0, 0 < \lambda_\phi \leq \sqrt{3}, \sqrt{\frac{6\lambda_\phi^2}{6 - \lambda_\phi^2}} \geq 2\delta$ or $0 < \delta \leq \sqrt{\frac{3}{2}}, \lambda_\phi > \sqrt{3}$ or $0 < \lambda_\phi < \sqrt{3}, 2\delta \geq \sqrt{6}$ or $\sqrt{3} < \lambda_\phi < \sqrt{6}, \sqrt{\frac{6\lambda_\phi^2}{6 - \lambda_\phi^2}} \leq 2\delta$

TABLE I: Fixed points of the autonomous equations (4.12) - (4.15).

of autonomous equations:

$$\frac{dx_1}{dN} = \frac{\sqrt{6}}{2}\lambda_\phi x_2^2 - 3x_1 - x_1 \frac{\dot{H}}{H^2}, \quad (4.12)$$

$$\frac{dx_2}{dN} = -\frac{\sqrt{6}}{2}\lambda_\phi x_1 x_2 - x_2 \frac{\dot{H}}{H^2}, \quad (4.13)$$

$$\frac{dx_3}{dN} = \frac{\sqrt{6}}{2}\delta(1 - x_1^2 - x_2^2 + x_3^2 - x_4^2) - 3x_3 - x_3 \frac{\dot{H}}{H^2}, \quad (4.14)$$

$$\frac{dx_4}{dN} = -2x_4 - x_4 \frac{\dot{H}}{H^2}, \quad (4.15)$$

where $\lambda_\phi \equiv -V_{,\phi}/\kappa V$. For an exponential form of a potential, i.e. $V(\phi) = V_0 e^{-\kappa\lambda_\phi\phi}$, λ_ϕ is a constant. Then the autonomous equations are closed.

Fixed points of the system can be obtained by setting $dx_1/dN = dx_2/dN = dx_3/dN = dx_4/dN = 0$. They are shown in Table I.

The dynamical variables x_2 and x_4 are always positive, while x_1 and x_3 can be positive or negative depending on the signs of $\dot{\phi}$ or $\dot{\sigma}$. We are interested only in the case where $\lambda_\phi > 0$ (an exponential decay) and $\delta > 0$. With these fixed points, density parameters and equation of state parameters are represented in Table II.

Fixed point (a) is a kinetic-dominated point. Radiation dominated epoch can be realized by the fixed point (b), (c), (e), or (f) because $w_{\text{eff}} = 1/3$. Fixed point (b) is a standard radiation dominated era, whereas other points

are mixture of radiation and other components. Point (d) or (h) can possibly be a matter dominated point, where both of them also have a dark energy component in the matter dominated epoch. The accelerated expansion era can be realized by point (g) or (h). Fixed point (g) is an accelerating expansion fixed point arising in the quintessence model, whereas point (h) is a scaling solution (i.e. a ratio of matter and dark energy is not equal to zero at late-time). Fixed point (d) cannot be an accelerating solution because the dark energy density is not

	Ω_m	Ω_r	Ω_{DE}	w_{DE}	w_{eff}
(a)	0	0	1	1	1
(b)	0	1	0	—	$\frac{1}{3}$
(c)	$-\frac{1}{3\delta^2}$	$1 + \frac{1}{2\delta^2}$	$-\frac{1}{6\delta^2}$	1	$\frac{1}{3}$
(d)	$1 + \frac{2\delta^2}{3}$	0	$-\frac{2\delta^2}{3}$	1	$-\frac{2\delta^2}{3}$
(e)	0	$1 - \frac{4}{\lambda_\phi^2}$	$\frac{4}{\lambda_\phi^2}$	$\frac{1}{3}$	$\frac{1}{3}$
(f)	$-\frac{1}{3\delta^2}$	$1 + \frac{1}{2\delta^2} - \frac{4}{\lambda_\phi^2}$	$-\frac{1}{6\delta^2} + \frac{4}{\lambda_\phi^2}$	$\frac{8\delta^2 - \lambda_\phi^2}{24\delta^2 - \lambda_\phi^2}$	$\frac{1}{3}$
(g)	0	0	1	$-1 + \frac{\lambda_\phi^2}{3}$	$-1 + \frac{\lambda_\phi^2}{3}$
(h)	$\frac{(\lambda_\phi^2 - 3)(3\lambda_\phi^2 + 2\delta^2(\lambda_\phi^2 - 6))}{3(\lambda_\phi^2 - 2\delta^2)^2}$	0	$\frac{12\delta^4 + 9\lambda_\phi^2 - 2\delta^2(18 - 3\lambda_\phi^2 + \lambda_\phi^4)}{3(\lambda_\phi^2 - 2\delta^2)^2}$	$\frac{2\delta^2(2\delta^2 - \lambda_\phi^2)(\lambda_\phi^2 - 3)}{12\delta^4 + 9\lambda_\phi^2 - 2\delta^2(18 - 3\lambda_\phi^2 + \lambda_\phi^4)}$	$\frac{2\delta^2(\lambda_\phi^2 - 3)}{6\delta^2 - 3\lambda_\phi^2}$

TABLE II: Density parameters and equation of state parameters of each fixed point.

negative at the present.

In the next section, stability of each fixed point will be examined by considering their corresponding eigenvalues.

B. Stability

The autonomous equations can be rewritten as

$$\begin{aligned}
\frac{dx_1}{dN} &= \mathcal{F}(x_1, x_2, x_3, x_4), \\
\frac{dx_2}{dN} &= \mathcal{G}(x_1, x_2, x_3, x_4), \\
\frac{dx_3}{dN} &= \mathcal{H}(x_1, x_2, x_3, x_4), \\
\frac{dx_4}{dN} &= \mathcal{I}(x_1, x_2, x_3, x_4).
\end{aligned}$$

Stability of the fixed points will be investigated by using the linear perturbation analysis around each fixed point, $(x_1^{(c)}, x_2^{(c)}, x_3^{(c)}, x_4^{(c)})$, by setting

$$x_i(N) = x_i^{(c)} + \delta x_i(N),$$

where $i = 1, 2, 3, 4$. The perturbation equations then take the form

$$\frac{d}{dN} \begin{pmatrix} \delta x_1 \\ \delta x_2 \\ \delta x_3 \\ \delta x_4 \end{pmatrix} = \mathcal{M} \begin{pmatrix} \delta x_1 \\ \delta x_2 \\ \delta x_3 \\ \delta x_4 \end{pmatrix}, \quad (4.16)$$

where the matrix \mathcal{M} is given by

$$\mathcal{M} = \begin{pmatrix} \frac{\partial \mathcal{F}}{\partial x_1} & \frac{\partial \mathcal{F}}{\partial x_2} & \frac{\partial \mathcal{F}}{\partial x_3} & \frac{\partial \mathcal{F}}{\partial x_4} \\ \frac{\partial \mathcal{G}}{\partial x_1} & \frac{\partial \mathcal{G}}{\partial x_2} & \frac{\partial \mathcal{G}}{\partial x_3} & \frac{\partial \mathcal{G}}{\partial x_4} \\ \frac{\partial \mathcal{H}}{\partial x_1} & \frac{\partial \mathcal{H}}{\partial x_2} & \frac{\partial \mathcal{H}}{\partial x_3} & \frac{\partial \mathcal{H}}{\partial x_4} \\ \frac{\partial \mathcal{I}}{\partial x_1} & \frac{\partial \mathcal{I}}{\partial x_2} & \frac{\partial \mathcal{I}}{\partial x_3} & \frac{\partial \mathcal{I}}{\partial x_4} \end{pmatrix} \bigg|_{x_1^{(c)}, x_2^{(c)}, x_3^{(c)}, x_4^{(c)}}.$$

Each component of the matrix \mathcal{M} is given in Appendix B.

The first order coupled differential equation (4.16) has a general solution

$$\delta x_i \propto e^{\mu N},$$

where μ is an eigenvalue of the matrix \mathcal{M} . Thus, if all eigenvalues are negative (or their real parts are negative for complex eigenvalues), the fixed point is stable. If at least one eigenvalue is positive, the fixed point is a saddle point. When all of eigenvalues are positive, the fixed point is unstable. Eigenvalues of each fixed point in Table I are as the following.

1. Fixed Point (a)

Eigenvalues of the fixed point are

$$\mu_{(a)} = 1, 0, 3 \pm \sqrt{6} \delta \sqrt{x_1^2 - 1}, 3 - \sqrt{\frac{3}{2}} \lambda_\phi x_1. \quad (4.17)$$

Although a sign \pm depends on roots of the condition $x_1^2 - x_3^2 = 1$, the fixed point is either saddle or unstable

point. Since this fixed point does not match with any known cosmological era, we no longer consider it.

2. Radiation Dominated Solutions

Eigenvalues of the fixed point (b), (c), (e), and (f) are given by

$$\mu_{(b)} = 2, -1, -1, 1. \quad (4.18)$$

$$\mu_{(c)} = -1, 2, -\frac{1}{2} \pm \frac{1}{2} \sqrt{-\left(\frac{2}{\delta^2} + 3\right)}, \quad (4.19)$$

$$\mu_{(e)} = -1, 1, -\frac{1}{2} \pm \sqrt{\frac{16}{\lambda_\phi^2} - \frac{15}{4}}, \quad (4.20)$$

$$\mu_{(f)} = -\frac{1}{2} \pm \frac{1}{2\delta^2\lambda_\phi^2} \sqrt{-\delta^2\lambda_\phi^4 + \delta^4(32\lambda_\phi^2 - 9\lambda_\phi^4) + \sqrt{\delta^4\lambda_\phi^4(\lambda_\phi^4 + 4\delta^4(16 - 3\lambda_\phi^2)^2 - 4\delta^2\lambda_\phi^2(16 + 3\lambda_\phi^2))}}, \quad (4.21)$$

$$-\frac{1}{2} \pm \frac{1}{2\delta^2\lambda_\phi^2} \sqrt{-\delta^2\lambda_\phi^4 + \delta^4(32\lambda_\phi^2 - 9\lambda_\phi^4) - \sqrt{\delta^4\lambda_\phi^4(\lambda_\phi^4 + 4\delta^4(16 - 3\lambda_\phi^2)^2 - 4\delta^2\lambda_\phi^2(16 + 3\lambda_\phi^2))}}. \quad (4.22)$$

Therefore, the fixed point (b), (c), and (e) are saddle points. For the point (f), we can understand the behaviour of the fixed point when we set the value of λ_ϕ and δ .

3. Matter Dominated Solutions

For the fixed point (d) and (h), their corresponding eigenvalues are

$$\mu_{(d)} = -\frac{3}{2} - \delta^2, -\frac{3}{2} - \delta^2, -\frac{1}{2} - \delta^2, \frac{3}{2} - \delta^2, \quad (4.23)$$

$$\begin{aligned} \mu_{(h)} = & \frac{\lambda_\phi^2 + 2\delta^2(\lambda_\phi^2 - 4)}{4\delta^2 - 2\lambda_\phi^2}, \frac{3\lambda_\phi^2 + 2\delta^2(\lambda_\phi^2 - 6)}{4\delta^2 - 2\lambda_\phi^2}, \\ & \frac{1}{4(\lambda_\phi^2 - 2\delta^2)^2} (-3\lambda_\phi^4 - 2\delta^2\lambda_\phi^2(\lambda_\phi^2 - 9) + 4\delta^4(\lambda_\phi^2 - 6)) \\ & \pm \sqrt{3(\lambda_\phi^2 - 2\delta^2)^2(72\lambda_\phi^2 - 21\lambda_\phi^4 + 4\delta^2(-72 + 18\lambda_\phi^2 + \lambda_\phi^4) + 4\delta^4(60 - 28\lambda_\phi^2 + 3\lambda_\phi^4))}. \end{aligned} \quad (4.24)$$

The fixed point (d) is stable when $\delta^2 > \frac{3}{2}$, whereas it is a saddle point when $\delta^2 < \frac{3}{2}$. For the fixed point (h), the eigenvalues can be understood once we set the value of λ_ϕ and δ .

4. Accelerated Expansion Solutions

Eigenvalues of the fixed point (g) are

$$\mu_{(g)} = \frac{1}{2}(\lambda_\phi^2 - 6), \frac{1}{2}(\lambda_\phi^2 - 6), \frac{1}{2}(\lambda_\phi^2 - 4), \lambda_\phi^2 - 3. \quad (4.25)$$

Thus, the fixed point is stable when $\lambda_\phi^2 < 3$. For the point (h) it is the same as the previous case.

Next we will solve the set of autonomous equations by numerical method.

V. NUMERICAL SOLUTIONS

In this section, the autonomous equations (4.12) - (4.14) are solved numerically, where we set $\lambda_\phi = 0.1$ and $\delta = 0.18$. Evolution of the density parameters and the equation of state parameters are shown in Fig 2.

Figure 2 demonstrates a viable cosmological scenario where the Universe evolved from the radiation dominated era to the matter dominated epoch, and followed by the late-time accelerated expansion. Since $\lambda_\phi = 0.1$ and $\delta = 0.18$, the fixed points (e), (f), and (h) do not exist, while the fixed point (c) yields $\Omega_r \approx 16.4$ which is too large. Since we are interested in $\Omega_r \approx 1$, we choose initial condition closed to the fixed point (b). The matter dominated era is point (d) automatically, and the accelerated expansion is the point (g). Therefore, the cosmological

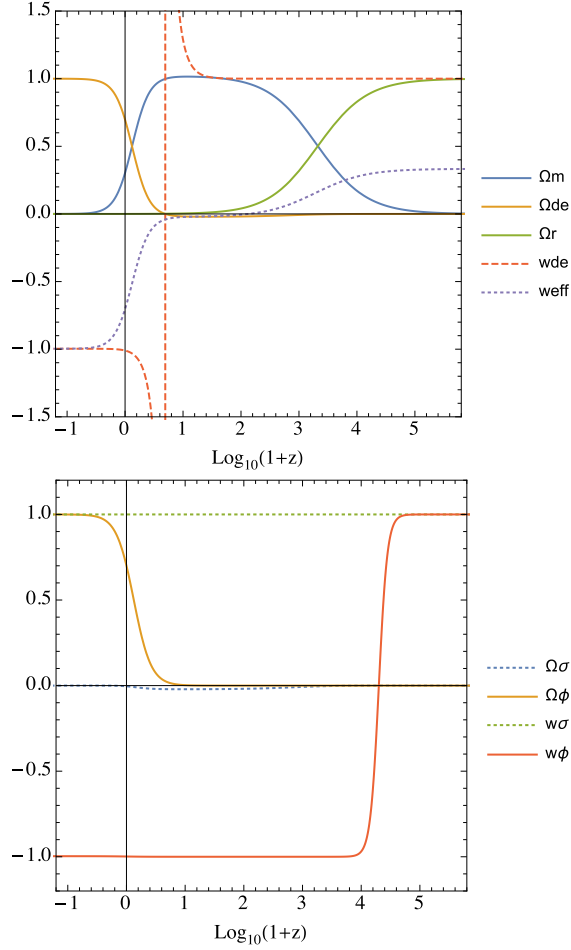


FIG. 2: Evolution of the density parameters and the equation of state parameters according to Eqs. (4.2) - (4.10) where initial conditions are $x_1 = 1 \times 10^{-5}$, $x_2 = 1 \times 10^{-10}$, $x_3 = 1 \times 10^{-5}$, and $x_4 = 0.9989$ at $z = 9.27 \times 10^6$.

viable evolution is

$$(b) \rightarrow (d) \rightarrow (g). \quad (5.1)$$

According to the bottom figure of Fig 2, the density of the phantom scalar field is negative and $w_\sigma = 1$ as desired, while the density of dark energy (quintessence + phantom) increases at late-time. We can obtain the evolution of the Hubble parameter by integrating Eq. (4.11),

$$H(N) = C \exp \left[\frac{1}{2} \left(-3N - 3 \int x_1^2 dN + 3 \int x_2^2 dN + 3 \int x_3^2 dN - \int x_4^2 dN \right) \right], \quad (5.2)$$

where C is a constant of integration which can be obtained by comparing the above equation to the Hubble parameter from the Λ CDM at the last-scattering surface. x_1 , x_2 , x_3 , and x_4 are obtained from numerical solutions with the same initial conditions used in Fig 2. We set $H_0 = 67.4$ km/s/Mpc to find the Hubble parameter at $z = 1100$ with the Λ CDM model, and then we

start the evolution in the quintom model from this value of $H(1100)$. The evolution of Hubble parameter of the quintom compared to that of the Λ CDM is shown in Fig 3.

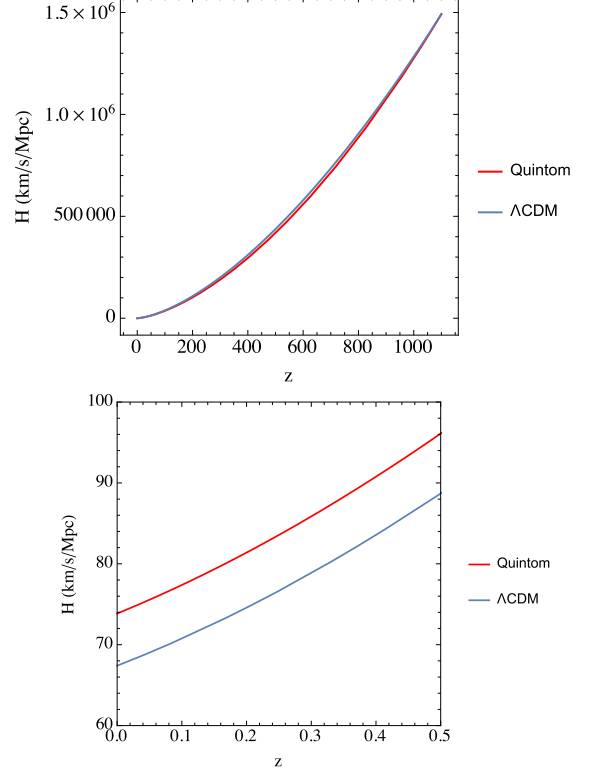


FIG. 3: Evolutions of the Hubble parameters, where top figure represents from $z = 1100$ (last-scattering surface) to the present time, while the bottom figure represents values at the late-time.

In Fig 3, the Hubble parameter of the quintom model decreases at slightly different rate comparing to the Λ CDM, where we find $H_0 = 73.85$ km/s/Mpc at the present time. Remarkably, the Hubble tension is resolved. Note that the value of H_0 depends on the initial conditions and the values of λ_ϕ and δ which can be tuned to provide better precision comparing to the observations. However, in this work we simply present a new method to solve the Hubble tension without seriously tuning the parameters.

Cosmological parameters at the present time obtained from numerical simulations are represented in Table III. These parameters correspond to the redshift at $z = 0$ in Figs 2 and 3.

VI. COMPARISON WITH DATA

In this section we would like to compare the evolution of Hubble parameter obtained by the quintom model with the observational data. We use observational data of Type Ia Supernovae at $z \geq 1$ from Table 6 of Ref. [36]

$\Omega_m^{(0)}$	$\Omega_{DE}^{(0)}$	$\Omega_r^{(0)}$	$\Omega_\sigma^{(0)}$	$\Omega_\phi^{(0)}$
0.304	0.696	9.45×10^{-5}	-0.004	0.70
w_{DE}	w_{eff}	w_σ	w_ϕ	
-1.01	-0.70	1	-0.998	

TABLE III: Cosmological parameters at the present time from the quintom model.

between the distance modulus μ_L and the redshift parameter. The data is known to be fit well by the Λ CDM model so it is a good place to check the validity of our coupled quintom cosmology. The distance modulus is related to the luminosity distance d_L by

$$\mu_L = 5 \log_{10} \left(\frac{d_L}{\text{Mpc}} \right) + 25. \quad (6.1)$$

The luminosity distance contains information of the evolution of the Universe through the Hubble parameter,

$$d_L = c(1+z) \int_0^z \frac{dz}{H(z)}, \quad (6.2)$$

where $H(z)$ can be calculated from Eq. (2.1) and Eq. (5.2) depending on the model. For the Λ CDM and other non-coupled phenomenological models, Eq. (2.1) is suffice. On the other hand, our quintom model with phantom-matter coupling can be more accurately calculated using Eq. (5.2). Figure 4 shows the comparison

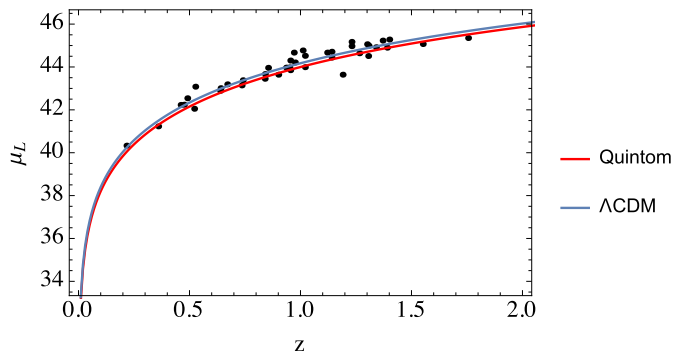


FIG. 4: Comparison between Type Ia Supernovae data from Ref. [36] and theoretical models: Λ CDM and quintom model.

son between theoretical models and the Supernovae observational data. The fitting of Λ CDM appears to be marginally better than the quintom model but both are good fits.

VII. CONCLUSIONS AND DISCUSSIONS

In this work, the Hubble tension is resolved by addition of a very small negative density component to the Uni-

verse. Such small contribution does not change the values $\Omega_m^{(0)} \simeq 0.31, \Omega_{DE}^{(0)} \simeq 0.69$ constrained by the Planck's CMB observation from the early Universe. As a realization of the idea, we consider a quintom model with conformal phantom-matter coupling and self-interacting quintessence that gives a viable cosmological scenario with the correct density parameters. The model satisfies the general phenomenological conditions, i.e., starting with radiation dominated era, continuing with matter and dark energy dominated era subsequently. It also contains the phantom crossing and finally resolves the Hubble tension, giving $H_0 = 73.85$ km/s/Mpc and $\Omega_m^{(0)} = 0.304, \Omega_\phi^{(0)} = 0.700, \Omega_\sigma^{(0)} = -0.004$ as shown in Table III.

Phenomenologically, as discussed in Section II, the required negative density of the extra component X for $w_X = 1$ is $\Omega_X^{(0)} = -4.708 \times 10^{-11}$, this is based on the non-coupled assumption of X to normal matter. In our quintom model, the conformal phantom-matter coupling is introduced in order to control the size of the negative density of the phantom field σ . In this coupled model, the negative density of the phantom field becomes $\Omega_\sigma^{(0)} = -0.004$ for $w_\sigma = 1$.

Acknowledgements

S.P. (first author) is supported by Rachadapisek Sompotte Fund for Postdoctoral Fellowship, Chulalongkorn University. P.B. is supported in part by the Thailand Research Fund (TRF), Office of Higher Education Commission (OHEC) and Chulalongkorn University under grant RSA6180002.

Appendix A: Effective potential

Considering the equation of motion of the phantom scalar field

$$\ddot{\sigma} + 3H\dot{\sigma} = \kappa\delta\rho_m. \quad (A1)$$

We introduce a conserved matter density as

$$\rho_m = \rho_m^{(c)} e^{\kappa\delta\sigma}, \quad (A2)$$

where a superscript (c) means a conserved quantity. Thus, the equation of motion can be rewritten as

$$\ddot{\sigma} + 3H\dot{\sigma} - \frac{\partial}{\partial\sigma} \left(\rho_m^{(c)} e^{\kappa\delta\sigma} \right) = 0. \quad (A3)$$

Obviously, the last term acts as an effective potential. Substituting this conserved matter density into the continuity equation (3.14), we find

$$\dot{\rho}_m^{(c)} + 3H\rho_m^{(c)} = 0. \quad (A4)$$

Therefore the matter density is conserved. This kind of the effective potential can be found in the chameleon

gravity or symmetron gravity [29, 33, 34]. However, we are not interested in the conserved matter density, but we would like to see dynamics of ρ_m which is influenced by the coupling δ .

Appendix B: Components of the matrix \mathcal{M}

For the autonomous equations (4.12) - (4.14), components of the matrix \mathcal{M} are as follows

$$\begin{aligned}
\frac{\partial \mathcal{F}}{\partial x_1} &= \frac{1}{2}(-3 + 9x_1^2 - 3x_2^2 - 3x_3^2 + x_4^2), \\
\frac{\partial \mathcal{F}}{\partial x_2} &= -3x_1x_2 + \sqrt{6}x_2\lambda_\phi, \quad \frac{\partial \mathcal{F}}{\partial x_3} = -3x_1x_3, \\
\frac{\partial \mathcal{F}}{\partial x_4} &= x_1x_4, \\
\frac{\partial \mathcal{G}}{\partial x_1} &= 3x_1x_2 - \sqrt{\frac{3}{2}}x_2\lambda_\phi, \\
\frac{\partial \mathcal{G}}{\partial x_2} &= \frac{1}{2}(3 + 3x_1^2 - 9x_2^2 - 3x_3^2 + x_4^2 - \sqrt{6}x_1\lambda_\phi), \\
\frac{\partial \mathcal{G}}{\partial x_3} &= -3x_2x_3, \quad \frac{\partial \mathcal{G}}{\partial x_4} = x_2x_4, \\
\frac{\partial \mathcal{H}}{\partial x_1} &= x_1(3x_3 - \sqrt{6}\delta), \quad \frac{\partial \mathcal{H}}{\partial x_2} = -x_2(3x_3 + \sqrt{6}\delta), \\
\frac{\partial \mathcal{H}}{\partial x_3} &= \frac{1}{2}(-3 + 3x_1^2 - 3x_2^2 - 9x_3^2 + x_4^2 + 2\sqrt{6}x_3\delta), \\
\frac{\partial \mathcal{H}}{\partial x_4} &= x_4(x_3 - \sqrt{6}\delta), \\
\frac{\partial \mathcal{I}}{\partial x_1} &= 3x_1x_4, \quad \frac{\partial \mathcal{I}}{\partial x_2} = -3x_2x_4, \quad \frac{\partial \mathcal{I}}{\partial x_3} = -3x_3x_4, \\
\frac{\partial \mathcal{I}}{\partial x_4} &= \frac{1}{2}(-1 + 3x_1^2 - 3x_2^2 - 3x_3^2 + 3x_4^2).
\end{aligned}$$

-
- [1] A. G. Riess *et al.* [Supernova Search Team], *Astron. J.* **116**, 1009 (1998) doi:10.1086/300499 [astro-ph/9805201].
 - [2] S. Perlmutter *et al.* [Supernova Cosmology Project Collaboration], *Astrophys. J.* **517**, 565 (1999) doi:10.1086/307221 [astro-ph/9812133].
 - [3] G. W. Horndeski, *Int. J. Theor. Phys.* **10**, 363 (1974). doi:10.1007/BF01807638
 - [4] C. Deffayet, X. Gao, D. A. Steer and G. Zahariade, *Phys. Rev. D* **84**, 064039 (2011) doi:10.1103/PhysRevD.84.064039 [arXiv:1103.3260 [hep-th]].
 - [5] T. Kobayashi, M. Yamaguchi and J. Yokoyama, *Prog. Theor. Phys.* **126**, 511 (2011) doi:10.1143/PTP.126.511 [arXiv:1105.5723 [hep-th]].
 - [6] L. Heisenberg, *JCAP* **1405**, 015 (2014) doi:10.1088/1475-7516/2014/05/015 [arXiv:1402.7026 [hep-th]].
 - [7] A. De Felice, L. Heisenberg, R. Kase, S. Mukohyama, S. Tsujikawa and Y. I. Zhang, *JCAP* **1606**, no. 06, 048 (2016) doi:10.1088/1475-7516/2016/06/048 [arXiv:1603.05806 [gr-qc]].
 - [8] C. de Rham, G. Gabadadze and A. J. Tolley, *Phys. Rev. Lett.* **106**, 231101 (2011) doi:10.1103/PhysRevLett.106.231101 [arXiv:1011.1232 [hep-th]].
 - [9] C. de Rham and G. Gabadadze, *Phys. Rev. D* **82**, 044020 (2010) doi:10.1103/PhysRevD.82.044020 [arXiv:1007.0443 [hep-th]].
 - [10] B. P. Abbott *et al.* [LIGO Scientific and Virgo Collaborations], *Phys. Rev. Lett.* **116**, no. 6, 061102 (2016) doi:10.1103/PhysRevLett.116.061102 [arXiv:1602.03837 [gr-qc]].
 - [11] B. P. Abbott *et al.* [LIGO Scientific and Virgo Collaborations], *Phys. Rev. Lett.* **119**, no. 16, 161101 (2017) doi:10.1103/PhysRevLett.119.161101 [arXiv:1710.05832 [gr-qc]].
 - [12] T. Baker, E. Bellini, P. G. Ferreira, M. Lagos, J. Noller and I. Sawicki, *Phys. Rev. Lett.* **119**, no. 25, 251301 (2017) doi:10.1103/PhysRevLett.119.251301

- [arXiv:1710.06394 [astro-ph.CO]].
- [13] J. Sakstein and B. Jain, *Phys. Rev. Lett.* **119**, no. 25, 251303 (2017) doi:10.1103/PhysRevLett.119.251303 [arXiv:1710.05893 [astro-ph.CO]].
- [14] P. A. R. Ade *et al.* [Planck Collaboration], *Astron. Astrophys.* **594**, A13 (2016) doi:10.1051/0004-6361/201525830 [arXiv:1502.01589 [astro-ph.CO]].
- [15] A. G. Riess, S. Casertano, W. Yuan, L. M. Macri and D. Scolnic, *Astrophys. J.* **876**, no. 1, 85 (2019) doi:10.3847/1538-4357/ab1422 [arXiv:1903.07603 [astro-ph.CO]].
- [16] K. C. Wong *et al.*, arXiv:1907.04869 [astro-ph.CO].
- [17] G. C.-F. Chen *et al.*, arXiv:1907.02533 [astro-ph.CO].
- [18] W. L. Freedman *et al.*, arXiv:1907.05922 [astro-ph.CO].
- [19] J. Renk, M. Zumalacregui, F. Montanari and A. Barreira, *JCAP* **1710**, no. 10, 020 (2017) doi:10.1088/1475-7516/2017/10/020 [arXiv:1707.02263 [astro-ph.CO]].
- [20] N. Khosravi, S. Baghran, N. Afshordi and N. Altamirano, *Phys. Rev. D* **99**, no. 10, 103526 (2019) doi:10.1103/PhysRevD.99.103526 [arXiv:1710.09366 [astro-ph.CO]].
- [21] E. Di Valentino, E. V. Linder and A. Melchiorri, *Phys. Rev. D* **97**, no. 4, 043528 (2018) doi:10.1103/PhysRevD.97.043528 [arXiv:1710.02153 [astro-ph.CO]].
- [22] V. Poulin, T. L. Smith, T. Karwal and M. Kamionkowski, *Phys. Rev. Lett.* **122**, no. 22, 221301 (2019) doi:10.1103/PhysRevLett.122.221301 [arXiv:1811.04083 [astro-ph.CO]].
- [23] K. Vattis, S. M. Koushiappas and A. Loeb, *Phys. Rev. D* **99**, no. 12, 121302 (2019) doi:10.1103/PhysRevD.99.121302 [arXiv:1903.06220 [astro-ph.CO]].
- [24] C. D. Kreisch, F. Y. Cyr-Racine and O. Dor, arXiv:1902.00534 [astro-ph.CO].
- [25] K. Dutta, Ruchika, A. Roy, A. A. Sen and M. M. Sheikh-Jabbari, arXiv:1808.06623 [astro-ph.CO].
- [26] S. Panpanich and P. Burikham, *Phys. Rev. D* **98**, no. 6, 064008 (2018) doi:10.1103/PhysRevD.98.064008 [arXiv:1806.06271 [gr-qc]].
- [27] Z. K. Guo, Y. S. Piao, X. M. Zhang and Y. Z. Zhang, *Phys. Lett. B* **608**, 177 (2005) doi:10.1016/j.physletb.2005.01.017 [astro-ph/0410654].
- [28] A. Naruko, D. Yoshida and S. Mukohyama, *Class. Quant. Grav.* **33**, no. 9, 09LT01 (2016) doi:10.1088/0264-9381/33/9/09LT01 [arXiv:1512.06977 [gr-qc]].
- [29] K. Hinterbichler, J. Khoury, A. Levy and A. Matas, *Phys. Rev. D* **84**, 103521 (2011) doi:10.1103/PhysRevD.84.103521 [arXiv:1107.2112 [astro-ph.CO]].
- [30] E. N. Saridakis and M. Tsoukalas, *Phys. Rev. D* **93**, no. 12, 124032 (2016) doi:10.1103/PhysRevD.93.124032 [arXiv:1601.06734 [gr-qc]].
- [31] L. Amendola, *Phys. Rev. D* **62**, 043511 (2000) doi:10.1103/PhysRevD.62.043511 [astro-ph/9908023].
- [32] S. Tsujikawa, doi:10.1007/978-90-481-8685-3_8 arXiv:1004.1493 [astro-ph.CO].
- [33] J. Khoury and A. Weltman, *Phys. Rev. Lett.* **93**, 171104 (2004) doi:10.1103/PhysRevLett.93.171104 [astro-ph/0309300].
- [34] J. Khoury and A. Weltman, *Phys. Rev. D* **69**, 044026 (2004) doi:10.1103/PhysRevD.69.044026 [astro-ph/0309411].
- [35] N. Aghanim *et al.* [Planck Collaboration], arXiv:1807.06209 [astro-ph.CO].
- [36] A. G. Riess *et al.*, *Astrophys. J.* **659**, 98 (2007) doi:10.1086/510378 [astro-ph/0611572].